Astron. Astrophys. 238, 485–493 (1990)

ASTRONOMY AND ASTROPHYSICS

Optimum weighting function in bispectral analysis in speckle interferometry: binary star parity detection

S.N. Karbelkar[1,2]

[1] Raman Research Institute, Bangalore 560 080, India
[2] Joint Astronomy Programme, Physics Department, Indian Institute of Science, Bangalore 560 012, India

Received January 9, accepted February 27, 1990

Abstract. In a previous paper (Karbelkar, 1990a) the SNR for detecting the parity of a binary star using the triple correlation was worked out on the basis of an idealized model of a speckle pattern. The calculations presented in this paper are based on a better description of the atmospheric noise and justify these approximations. The important issue of the relative merit of different bispectral regions is discussed in the specific context of binary star parity detection.

Key words: speckle interferometry – image processing – seeing

1. Introduction

It is well-known that the atmospheric turbulence limits the resolution of the long exposure images formed using ground-based large telescopes (for a recent review see Roddier, 1988). Random refractive index inhomogeneities, associated with the turbulent atmosphere, give rise to complex modulation of the stellar light as it passes through the atmosphere. As a consequence the point spread function (PSF) contains many bright spots – the so called speckles. These speckles have nearly diffraction limited size and they are spread over a (much wider) seeing disk about 1″. As the atmospheric conditions change with time (typical timescale 10 ms) the speckle pattern changes and on long exposure one records only the envelop seeing disk for a point source. Although the speckle pattern is quite random two nearby point sources will produce similar images as the light from these sources encounters almost the same turbulent regions. This so called isoplanatic patch is about 10″ in the optical.

The correlations in the speckle images of a complex source (smaller than the isoplanatic patch) form the basis of speckle interferometry, a ground based high resolution technique. Labeyrie (1970) proposed and Gezari et al. (1972) demonstrated the use of the power spectrum of the speckle image in measuring stellar diameter. The power spectrum, however, does not yield the phases of the object distribution. Measuring these phases is important if unambiguous object reconstructions are needed. Two promising phase reconstruction schemes exist. Knox and Thompson (1974) proposed the use of a second order correlation which gives the gradients of the object distribution. Nisenson and Papliolios (1983) were the first to investigate the effect of photon noise on image reconstruction using Knox-Thompson algorithm. Ayers et al. (1988) have considered the full four dimensional extension of the technique with a better description of the photonic and the atmospheric noise. The difference arising from the nature of the source has been pointed out recently (Karbelkar, 1990c) in the context of the Knox-Thompson algorithm itself (i.e. for the double correlation Knox-Thompson method).

Weigelt (1977) proposed a triple correlation (TC), the bispectrum, method of phase reconstruction. This method has been discussed in detail by Lohman et al. (1983). One of the interesting features of the bispectrum is that it contains as a subset the kind of correlations used in the Knox-Thompson method as well as genuine triple correlation. In this method the bispectrum forms an intermediate step; the object phases are obtained from the bispectrum values. A first realistic attempt to theoretically assess the potential of this method was made by Wirnitzer (1985). However, using an idealized approximation for the speckle pattern Karbelkar and Nityananda (1987) pointed out that the previous result overestimates the SNR in the high flux limit. Ayers et al. (1988), Hoffmann (1988), Karbelkar (1988) and Nakajima (1988) have pointed out that the previous results overestimate the SNR for low light levels as well. In their detailed analysis of the SNR properties of the bispectrum method Ayers et al. (1988) and Nakajima (1988) study the relative merits of different regions of the bispectrum for a point source. Karbelkar (1990a) has considered the specific case of parity detection (i.e. quadrant ambiguity removal) using the triple correlation method. In this analysis a simple model for the speckle pattern was used to reduce the complexity of calculating field-correlations of very high order. In addition the Knox-Thompson aspect of TC was neglected. These simplifications allowed a rather complete analysis of the noise properties of the technique valid at all light levels. In this paper we justify these approximation on the basis of a better description of the image correlations. In particular we show that, for binary separations close to the diffraction limit of the telescope, the genuine triple correlation aspect of the technique has a better SNR ratio than that for the near-axes Knox-Thompson aspect. This result appears to contradict the results by Ayers et al. (1988) and Nakajima (1988) who demonstrate, both analytically as well as numerically, that the near axes region in the triple correlation has a better SNR. The explanation lies in the fact that these authors consider only a point source while the present paper deals with a binary.

This paper is organised as follows. We work with the focal plane correlations instead of correlations in the spatial frequency domain. We first calculate the general triple correlation (as used

in speckle masking) for a point source. This is inversion symmetric about its center. We then calculate the triple correlation for a binary and show that the genuine triple correlation aspect is not a strong function of the binary separation but the SNR for Knox-Thompson subset of the TC depends linearly on the binary separation. This dependence makes the Knox-Thompson regions less important for complex sources with structure on the scale of the diffraction limit of the telescope. This result parallels the similar result for the KT (double correlation) proper mentioned above and strengthens the relation of the near axes region of the TC with the KT algorithm.

At low light levels it is necessary to consider the effect of photon noise. Goodman and Belsher (1976, 1977) were the first to consider the photon limited images and their restoration. Applying their method Wirnitzer (1985) has derived the unbiased estimator for the bispectrum. The variance on this estimator was derived by Ayers et al. (1988) and Nakajima (1988). In this paper we use a triple correlation which weights different parts of the triple correlation differently. An algorithm (Karbelkar, 1990b) which generalizes the approach of Goodman and Belsher (1967, 1977) has been used.

2. The triple correlation for a binary

In this paper we model atmospheric noise by using single scale Gaussian statistics for the pupil plane fields due to a point source. In reality, multiscale turbulence is known to result in randomly wandering centroid of a speckle image. This is attributed to large scale refractive index inhomogeneities which contribute to the overall tilt of the pupil plane wavefront. The effect of centroid shift has been considered by Ayers et al. (1988) and Beletic (1988) in their comparative study of the KT and the TC analysis. Beletic, in his numerical simulations, finds the TC to have better SNR for complex sources. He attributes the shortcomings of the KT method to the drifting nature of the centroid. A recent focal plane analysis by the author (Karbelkar, 1990c) brings out another reason why the KT method should perform poorer for complex sources. Here we briefly summarize the argument. Different speckles due to a point source can be considered to have uncorrelated intensities. In a speckle pattern for a binary every pixel receives two speckles: each one due to both stars. The intensity of these speckles are uncorrelated. However, two pixels separated by the binary separation will have a pair of speckles with the same relative intensity as the binary. Any information about the binary must come from this correlated pair of speckles (otherwise one can be happy with the long exposure image). Now, for the KT method to work finite size of the seeing disk is a must. If the telescope diameter were infinite in comparison with the Fried parameter then the speckle pattern would become stationary (statistically invariant under shifts) in the focal plane. As is well-known, the only nonvanishing double correlation for a stationary process is its power spectrum which does not contain any phase information. The statistics of the speckles change on the scales of the seeing disk and this change must be felt by the correlated pairs of speckles separated by the binary separations. Therefore, we expect a small factor b/σ in the SNR expression for this method. We note that for separations close to the diffraction limit this small parameter is $N_S^{-1/2}$. This dependence makes the KT method poorer for complex sources. We note that the TC technique, on the other hand, does not demand any such restriction on the values of the spatial frequencies. A process may be stationary and yet have nonvanishing triple correlation. However, it remains to be seen whether the TC method also has any dependence on the binary separation. In this section we answer this question.

2.1. The PSFTC

The triple correlation, as used in the speckle masking method, for a point source

$$T_R(Y,Z)=\int d^2X\langle R(X)R(X+Y)R(X+Z)\rangle. \quad (1)$$

is defined on the four dimensional space (Y_1, Y_2, Z_1, Z_2). Here $R(X)$ is the point spread function (PSF). We emphasize that in this paper we are dealing with focal plane triple correlation. As the name suggests it correlates intensity at three points. We have shown this PSFTC schematically in Fig. 1. In the (Y_1, Z_1) plane ((Y_2, Z_2) is similar) there are five features of this triple correlation. The feature A is a plateau region with extension of the order of the seeing disk. Then there are three ridges B, C and D with width of the order of speckle size and extension of the order of the seeing disk. In the full four dimensions these are actually planar layers (for example the feature B is the plane $Y=Z$). The layered nature comes about because the equalities are not exact but allow for a tolerance of the order of the speckle size. The feature E is located at the center of the four-space and has a size of the order of the speckle size. In our Gaussian model all these features have Gaussian fall-offs with above mentioned length scales. At the origin of the four space the feature E is twice as strong as other features (which have equal strengths at the origin). The strength at the origin can be readily estimated. With our normalization $\pi N_0 R^2$ is the total photon count per exposure for a zeroth magnitude star. This flux is spread all over the seeing disk of size $\sigma \sim f/kl$ where l is related to the Fried parameter. Thus the average focal plane intensity density is $\langle R\rangle = N_0 R^2 k^2 l^2/f^2$. For far away points in the seeing disk the three intensities entering the triple correlation will have statistically independent fluctuations so the scaling estimate for the triple correlation density for a

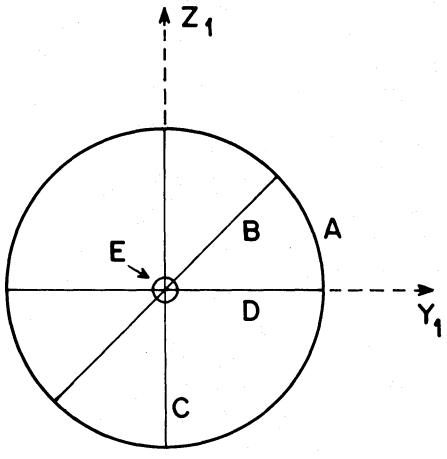

Fig. 1. The triple correlation for a point source shown schematically. It consists of the genuine triple correlation feature E, three correlation ridges B, C and D which are Knox-Thompson kind of regions of the triple correlation and the uncorrelated feature A

typical triple correlation element within a seeing size is

$$\int d^2X \langle R\rangle^3 \sim (f/kl)^2 \left(\frac{N_0 k^2 l^2 R^2}{f^2}\right)^3 = \frac{N_0^3 k^4 l^4 R^6}{f^4}. \quad (2)$$

This is precisely the term A arising from uncorrelated fluctuations in the three PSFs involved in the triple correlation. The ridges B, C and D appear because in this region of the triple correlation two (and only two) of the three points involved in the triple correlation are within a speckle size and thus have correlated intensity fluctuations. Thus in addition to the all pervading feature there is enhancement of the triple correlation. Finally the term E with weight two comes about because all the three points involved in triple correlation are within a speckle size. Note that the number of terms (counting E twice) is a reflection of the asymptotic Rayleigh distribution assumed in the Appendix B. In those regions where some of these terms are equal (even though they might have fallen off considerably from their peak values at the center) we see that for general element only one term, for ridges two terms, and near centre all six terms contribute. This is indicative of the Rayleigh asymptotic $\langle\mu\rangle = \langle\mu\rangle; \langle\mu^2\rangle = 2\langle\mu\rangle^2; \langle\mu^3\rangle = 6\langle\mu\rangle^3$ where μ is a Rayleigh variable with mean $\langle\mu\rangle$.

We note that of the three correlation ridge features B, C and D only one contains statistically independent information as the others are just two different ways of writing the same event. This is true in all realizations of atmospheric and photonic noise.

Let us call all the features (A, B, C, D, 2E) collectively a unit of triple correlation (short for triple correlation transfer function). For a binary the intensity $I(X)$ is given by

$$I(X) = \alpha_1 R(X) + \alpha_2 R(X-b), \quad (3)$$

where b is the binary separation, α_1 and α_2 represent the relative strengths of the component stars. We align the focal plane axes such that the binary is along the first axis with subscript 1. The triple correlation T_B for the binary can be written in terms of the same T_R for the zeroth magnitude point source

$$\begin{aligned} T_B(Y, Z) = (\alpha_1^3 + \alpha_2^3) T_R(Y, Z) + \alpha_1^2 \alpha_2 [T_R(Y, Z-b) \\ + T_R(Y-b, Z) + T_R(Y+b, Z+b)] \\ + \alpha_1 \alpha_2^2 [T_R(Y, Z+b) \\ + T_R(Y+b, Z) + T_R(Y-b, Z-b)]. \end{aligned} \quad (4)$$

It contains seven basic units with strengths and locations shown in Fig. 2. Note that this is just a convolution of the basic triple correlation unit (Fig. 1) and the triple correlation for the binary in the absence of atmospheric noise. Since the strengths of different units are asymmetric the triple correlation is also asymmetric and one has to extract the asymmetry in the best possible way. This leads to the interesting question of finding those regions of the four space which give better SNR for parity. Perhaps a more interesting question is to ask what is the relative importance of various features of the basic unit in determining parity. In Karbelkar (1990a) all the emphasis was on the feature E, i.e. the central region in the triple correlation transfer function. Since various features have negligible overlap volumewise, a superposition approximation for the signal and noise (of course separately) holds in that once we know what effect each kind of feature has one can figure out what weight function to use to get better SNR. So we consider the following three cases: (a) SNR due to the central feature alone [this was considered before

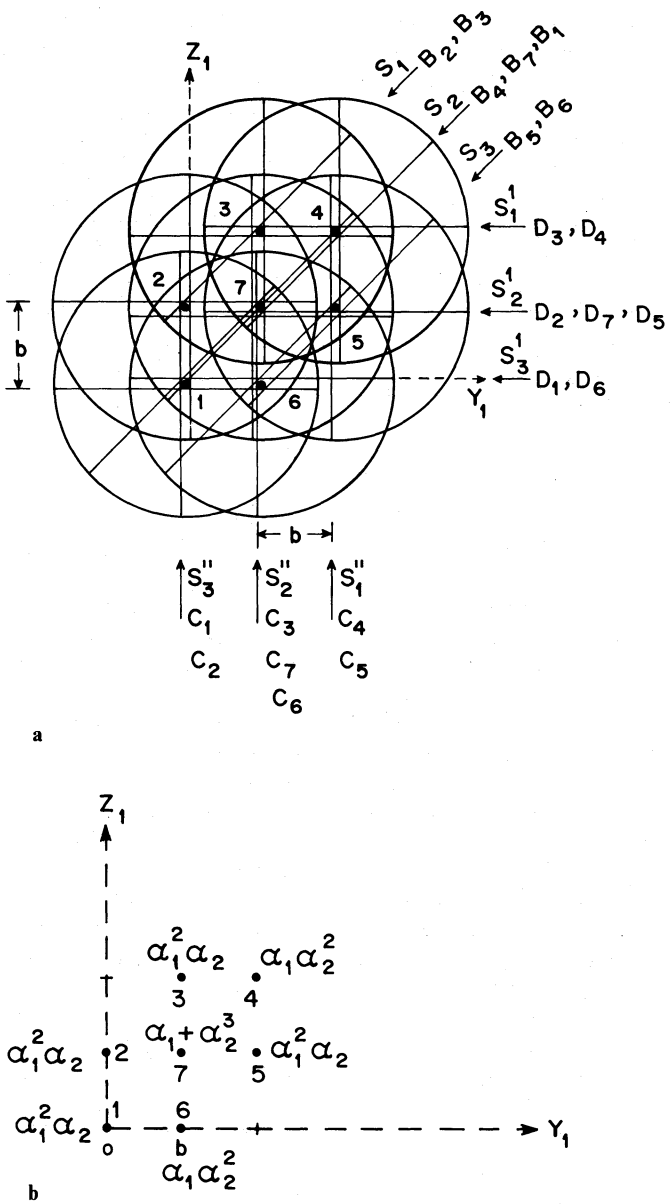

Fig. 2. a Triple correlation for a binary. It consists of seven PSFTCs. The ridges are shown slightly displaced for clarity. **b** The strengths of the seven PSFTCs forming the TC for the binary

(Karbelkar, 1990a) in detail], (b) the SNR due to the correlation ridges B, C and D, (c) the SNR due to the plateau feature A (long exposure case!).

At this stage it is possible to anticipate the separation dependence of the SNR for the parity detection using various features. Consider only the E-features. These are located at seven places in the triple correlation. Now, once the binary separation is slightly greater than a speckle size the asymmetry due to these features will be independent of the binary separation. As the binary separation increases, however, the noise due to the other features, which overlap with them, will decrease. The length scale for this change is of the order of the seeing disk and can be neglected (as one is interested in closer binaries). On the other hand, for other features one expects strong dependence on the separation. Consider the correlation ridges for example. As one is always

interested in separations much smaller than the extension of these features the signal will be proportional to the separation (the proportionality need not be linear as we shall see). This is for the following reason. We are interested in the asymmetry about the center of the triple correlation which coincides with the seventh PSFTC. The seventh PSFTC, therefore, does not contribute to any asymmetry (even if it were not on the center it won't because it is symmetric in the strength of the binary components). The other PSFTCs are away from the center and contribute to the asymmetry. However, the contribution is much less than their own strength because the part on one side of the center balances a large part on the other side. Only the E-features (due to the first six PSFTCs) are to the single side of the center of the binary triple correlation.

2.2. *Parity detection due to the feature E*

In the triple correlation for the binary the E-feature appears at seven places. The central one has a strength which is symmetric in the fluxes of the component stars and thus does not contain any parity information. As a consequence of the definition of the triple correlation only two of the remaining six E-features contain independent information. We choose the E-features of the first and the fourth PSFT to obtain an antisymmetric parity statistic. So our weight function of the first kind is shown in Fig. 3. It has two ports where it takes nonzero values and these ports have four volume equal to the feature. Note that though the weight function is mainly designed to pick up contribution due to the feature it also gets contribution from others. We label the seven PSFTCs as shown in Fig. 3. We can then denote the contribution of a specific feature due to a specific unit: for example, D_3 means the D-feature of the third unit which passes through the port 2. The overlap of any of the features A – D with the weight function results in an equivalent E-feature because the weight function has the four volume equal to the feature E. This is true as long as the binary separation is much smaller than the seeing. Otherwise, the other features would have fallen off considerably at the location of the two ports and the overlap would be weaker than the E-features located at the ports.

The parity statistic is of the form

$$\int d^2Y d^2Z\, W(Y, Z) T_B(Y, Z). \tag{5a}$$

The low light level variance is given by

$$2\int d^2Y d^2Z\, W(Y, Z)^2 T_B(Y, Z). \tag{5b}$$

This result follows from the general results on Poisson fluctuations. An application of the diagramatic rule (Karbelkar, 1990b) for the variance yields a total of 33 terms for the averaged squared modulus of a general triple correlation. These include a sixth order term, nine fifth order terms, eighteen fourth order terms and six third order terms. Because of the symmetry of the weight function and the triple correlation the six lowest order terms can be paired. This explains the factor two in the above expression. For a general weight function there are two more terms in this lowest order in intensities. If we had made no use of the fact that only two of the peripheral six E-features are independent and blindly used all the six asymmetric features then these other two terms in the variance expression mentioned above would have made sure that the variance is nine times as large thus leaving SNR unaffected (see Appendix A). To get the signal we weight the port 1 by $+1$ and the port 2 by -1 and add. We must also multiply by the four volume of the ports and the triple correlation density. Thus the parity signal due to the E-feature is

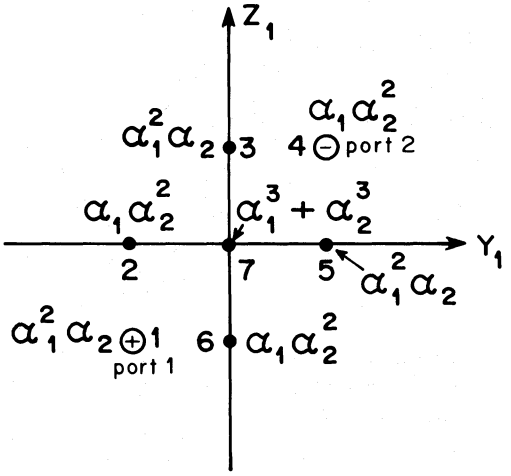

Fig. 3. The weight function used to emphasize the feature E

$$\begin{aligned} S_E &\sim 2\alpha_1\alpha_1(\alpha_1-\alpha_2)(f/kl)^4 (N_0^3 k^4 l^4 R^4/f^4) \\ &= 2\alpha_1\alpha_2(\alpha_1-\alpha_2)N_0^3 R^2 l^4 \\ &\sim 2\mathcal{N}_1\mathcal{N}_2(\mathcal{N}_1-\mathcal{N}_2)N_S, \end{aligned} \tag{6}$$

where $\mathcal{N}=(\alpha N_0 l^2/16)$ is the photon count per speckle in an exposure and N_S is the average number of speckles. The low light level variance is

$$\begin{aligned} V_E &\sim 2(4\alpha_1^3+14\alpha_1^2\alpha_2+14\alpha_1\alpha_2^2+4\alpha_2^3)(f/kR)^4 \frac{N_0^3 k^4 l^4 R^4}{f^4} \\ &\sim 4(2\alpha_1^3+7\alpha_1^2\alpha_2+7\alpha_1\alpha_2^2+2\alpha_2^3)N_0^3 l^2 R^2. \end{aligned} \tag{7}$$

The approximation is in using order of scaling estimates for the four volume of the E-feature and the triple correlation density. Thus the SNR for parity detection using the E-feature alone is

$$\begin{aligned} \mathrm{SNR}_E = &\frac{4}{3\sqrt{\pi}} q^{3/2} M^{1/2} N_S^{1/2} \\ &\times \frac{\mathcal{N}_1\mathcal{N}_2(\mathcal{N}_1-\mathcal{N}_2)}{[2\mathcal{N}_1^3+7\mathcal{N}_1^2\mathcal{N}_2+7\mathcal{N}_1\mathcal{N}_2^2+2\mathcal{N}_2^3]^{1/2}}. \end{aligned} \tag{8}$$

The scaling is the same as that given in Karbelkar (1990a). The numerical coefficient is provided by the Appendix A which evaluates quantities of interest exactly. As the binary separation increases we can see that the contribution to the noise from the feature remains constant but that due to all other terms falls off. The fall-off scale is, however, comparable to the seeing. We, therefore, conclude that SNR due to the feature is weakly dependent on the binary separation.

2.3. *SNR for parity detection due to correlation ridges*

Figure 2 shows regions of the (Y_1, Z_1) plane where correlation ridges exist. For clarity the ridges are shown slightly displaced, in

reality ridges like D_1 and D_6, for example, coincide in the region common to both. We see nine strips in this plane where correlation ridges from two or three triple correlation units overlap. Because of the symmetry of the triple correlation only two (to be precise 1.5) of these nine strips contain independent information. To see this, consider a strip with equation $Z=Y+C_0$. Then from the definition of the triple correlation the same strip appears at $Z=C_0$ and at $Y=C_0$:

$$\int d^2X I(X)I(X+Y)I(X+Z)=\int d^2X I(X-Y)I(X)I(X+C_0) \tag{9}$$

i.e. if the coordinates on the first strip are $(Y, Z=Y+C_0)$ then the same event is also written at $(-Y, Z=C_0)$. Figure 2 shows three strips S_1, S_2 and S_3 and their two copies each (denoted with a single and double primes). Note that the strips S_1, S_2 and S_3 have the same orientation as the B feature. In fact, for the PSFTC shown in Fig. 1 only one of the features B, C and D contains independent information. Further reduction in the number of ridges is due to the symmetry of the triple correlation under the interchange of Y and Z. Because of this symmetry the strips 1 and 3 are identical for every realization. In the following we have used all the three strips instead of using any one of the strips 1 and 3 and half of the second strip split lengthwise. Similar situation arose in the case of the double correlation analysis (Karbelkar, 1990c) where it was shown that both these schemes give the same SNR. In the present context also it can be shown that these schemes give the same SNR. Although the weight function is designed to emphasise B type feature it will also pick up contribution from the feature A. The weight function will also pick up contribution due to the feature E. For the reasons given later in Sect. 2.5 we need not consider it here. In Fig. 4a we show strips 1, and 2 in greater details. The centers and the strengths of these features are shown in the figure. We are interested in the leading contribution in powers of binary separation b. Consider the strip 1 for example. The unit 1 contributes to this strip via the A-feature. Now since the binary separation is assumed small one can think of the contribution due to the A feature on the strip to have effective center shown in the figure. In fact this is the center of the overlap between the feature and the strip. The overlap is equivalent to a feature B. In Fig. 4a the centers of such effective features are shown by smaller dots and these are linked to the centers of the original features by dotted lines. In Fig. 4b we see the centers and the strengths of such effective B features. We are interested in the asymmetry in these three strips. Because of the Y and Z symmetry of the triple correlation the lower half of the strip 1 is equivalent to the lower half of the strip 3 and so on. Thus asymmetry about the origin is equivalent to asymmetry of the individual strips about the $-45°$ line passing through the center. Figure 4c shows the effect of the special weight function $W(\eta)$ which is situated at a distance x away from the center of the effective feature $B(\eta)$. Only the contribution from the central region between $\pm x$ survives. So for a weight function of this kind contribution depends linearly on the distance of the jump in the weight function from the center of the feature under consideration. It turns out that strips 1 and 3, which are identical have their centers shifted from the $-45°$ line in the sense opposite to that of the middle strip which has its center shifted twice as much. This motivates our weight function shown in Fig. 5. The asymmetry in the triple correlation can be readily estimated when we note that the shift in the centers of the strips are of the order of b. We get the signal due to all the strips

$$S_B=\frac{\pi^{3/2}N_0^k l^3 R^4 b}{\sqrt{3}\,2^6 f}\alpha_1\alpha_2(\alpha_1-\alpha_2)$$
$$=\frac{2}{\sqrt{3}\pi^{1.5}}N_S^{3/2}q^3\mathcal{N}_1\mathcal{N}_2(\mathcal{N}_1-\mathcal{N}_2)B. \tag{10}$$

Here $B=kRb/f$ is the binary separation in units of speckle diameter.

For this weight function the variance calculation needs to be done to all orders to decide the low and high flux regimes. This is done in Appendix B using a simple PSF model described there.

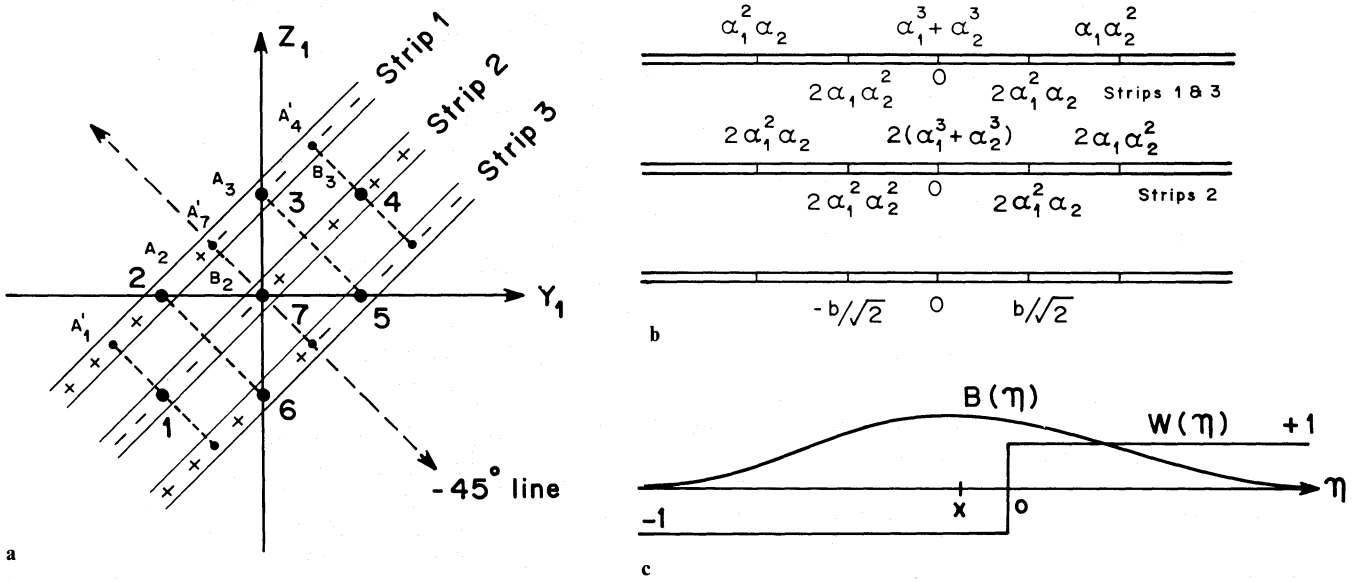

Fig. 4. a The weight function used to emphasize the correlation ridges. **b** The locations and the strengths of the equivalent B-features. **c** An effective B-feature $B(\eta)$ with center a distance x away from the jump in the weight function $w(\eta)$

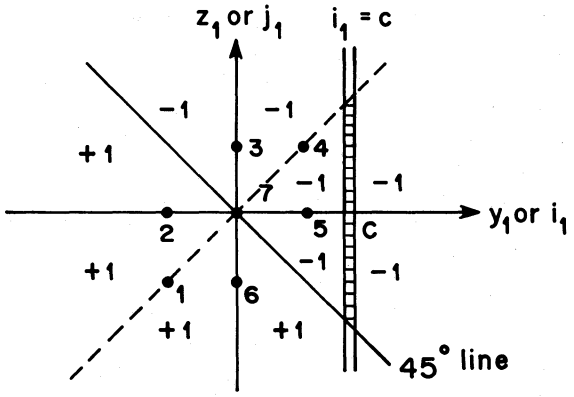

Fig. 5. The weight function used to emphasize the feature A

The result is

$$V_B = 24q^6(\mathcal{N}_1+\mathcal{N}_2)^6 N_S^3 + 4q^5(\mathcal{N}_1+\mathcal{N}_2)^5 N_S^3 + \frac{4}{3}q^4(\mathcal{N}_1+\mathcal{N}_2)^4 N_S^3 + 4q^3(\mathcal{N}_1+\mathcal{N}_2)^3 N_S^2. \quad (11)$$

We see that the transition to low flux goes through two steps. The first transition occurs for objects fainter than 13^m. The fourth order contribution takes over from the sixth order contribution which dominates at high light levels. The second transition occurs for objects fainter than 20^m. The third order contribution dominates for lower light levels. The first occurs when a speckle receives less than one photon in an exposure (13th magnitude) and the second when all speckles together receive less than one photon per exposure (20th magnitude). The SNR for parity detection using these correlation ridges is

$$SNR_B = \frac{\sqrt{2}}{3\pi^{1.5}} M^{1/2} \frac{\mathcal{N}_1\mathcal{N}_2(\mathcal{N}_1-\mathcal{N}_2)}{(\mathcal{N}_1+\mathcal{N}_2)^3} B \quad \text{high flux} \quad (12a)$$

$$= \frac{2}{\pi^{1.5}} q M^{1/2} \frac{\mathcal{N}_1\mathcal{N}_2(\mathcal{N}_1-\mathcal{N}_2)}{(\mathcal{N}_1+\mathcal{N}_2)^2} B \quad \text{medium flux} \quad (12b)$$

$$= \frac{2}{\sqrt{3}\pi^{1.5}} q^{3/2} N_S^{1/2} M^{1/2} \frac{\mathcal{N}_1\mathcal{N}_2(\mathcal{N}_1-\mathcal{N}_2)}{(\mathcal{N}_1+\mathcal{N}_2)^{3/2}} B \quad \text{low flux.} \quad (12c)$$

We note that for the objects of present day interest (brighter than 20th magnitude) and for close binaries the SNR due to the correlation ridges is never better than the SNR due to the main triple correlation feature E.

2.4. SNR for parity detection using the feature A

For +45° strips (parallel to the B-feature) other than the correlation ridges the asymmetry starts in the cubic order in the binary separation. If we approximate the near center strength of an effective B-feature by its peak value then for a general +45° strip contributions due to various triple correlation units cancel in the first order in b. One has to retain the quadratic near peak variation to get any asymmetry. Other reason for cubic asymmetry is that when the binary separation is large the extensions and the strengths of the features B and B′ (overlap of a feature A and a 45° strip) differ in the second order in the separation. In Fig. 5 we show a representative weight function of the third kind designed to emphasise the asymmetry due to the feature A. A straightforward calculation gives the signal for this weight function

$$S_A = \frac{\pi^{2.5}}{3^{1.5}2^{5.5}} N_0^3 \alpha_1\alpha_2(\alpha_1-\alpha_2) \frac{k^3 l^3 R^6 b^3}{f^3}. \quad (13)$$

The variance, in principle, needs to be evaluated up to all orders. However, contribution to the variance is positive in every order so even if we consider only the third order contribution to the variance:

$$V_{A3} = 1.5\pi^2 N_0^3(\alpha_1+\alpha_2)^3 R^6 \quad (14)$$

one gets an upper bound

$$SNR_A \leq \frac{16q^{3/2}M^{1/2}\mathcal{N}_1\mathcal{N}_2(\mathcal{N}_1-\mathcal{N}_2)}{9(\mathcal{N}_1+\mathcal{N}_2)^{3/2}} B^3 \quad (15)$$

on SNR. We note that even this upper bound is no match to the SNR due to the E feature for small binary separations. It is well-known that for large separations parity is better determined by using long exposure image. We, therefore, conclude that although for large binary separations the parity may be better determined by the A-feature it cannot be regarded as a genuine high resolution feature. Numerical results in this paper assume 1″ seeing, 10 ms exposure time, 4 m telescope and 100 Å bandwidth.

3. Discussion

Superposition approximation: So far we considered SNR for individual features like the central E-feature, the ridges and the feature A. We mentioned that a kind of superposition approximation enables one to consider these features independently. The reason is the great difference in the four volumes of various features. To be specific, if we take the four volume of the E-feature as unity then the four volumes of the ridges and the A feature are N_S and N_S^2 respectively. Now let us go back to SNR due to the feature E. The weight function used in this case had four volume equal to that of the feature. The parity signal is purely due to the E-feature and the noise comes from other features. For this reason one is justified in attributing the parity signal to the feature. Next, consider the weight function of the second kind used to emphasize the feature B. In this case the signal not only comes from the B-feature but also from the feature E. There are two reasons why we did not consider the contribution due to this feature in Sect. 2.4. The first reason is that its contribution is negligible when compared to that of the feature B. To see this consider the signal first. For concreteness we consider very low fluxes where signal and variance are proportional to the four volume involved. The contribution to the signal due to the E-feature is proportional to its four volume. The feature B has N_S times larger volume and although it suffers from "edge" effects (due to extension larger than the binary separation) which, as described in Sect. 2.4, subdue its contribution by a factor $N_S^{1/2}$ its signal is still $N_S^{1/2}$ times larger than that due to the E-feature. Unfortunately, the variance does not suffer from any "edge" effects and is larger by a factor N_S. In this case of very low fluxes (fainter than 20^m) the two features will have comparable SNR for close binaries. For flux levels of interest in speckle interferometry (between 13^m and 20^m) the SNR due to the E-feature is larger.

Even in this case one can arrive at the superposition approximation by redefining the weight function so that it excludes all E-features. For example, we may leave holes in the weight function at the locations of the E-features. This won't affect the previous estimates because the size of such holes is very much smaller than the volume of the entire weight function. For similar reasons one can omit the features B and E while considering parity due to the feature A.

Fine tuning the weight function: In this paper we considered a rather simple weight function. The weight function was either -1 or $+1$. It is certainly possible to improve the SNR by a smoother variation of the weight function. Intuitively, we would expect the optimum weight function to follow the signal. The weight function should be large where more signal comes from. However, we also know that within the fall off scales the signal is more or less uniform. Therefore, we do not expect a fine tuning of the weight function to change the scalings with $\mathcal{N}$, N_S and B although numerical coefficient may change a bit.

Effect of the Kolmogorov spectrum for the atmospheric inhomogeneities: The effect of the larger scales (comparable to or larger than the telescope pupil) in the turbulence is to tilt the entire wavefront. The speckle pattern will have its instantaneous centroid wandering. However, unlike the double correlation method the triple correlation does not share this focal plane motion of the speckle pattern. This is because the triple correlation defined in Eq. (5) is invariant under shifts in the focal plane.

Acknowledgement. It is a pleasure to thank Rajaram Nityananda for many useful discussions.

Appendix A: SNR calculations

Here we give the details of the SNR calculations described qualitatively in the text. We are not concerned with correlation effects due to secondary Airy rings in a real telescope so we use Gaussian apodization in the pupil plane. The focal plane field $\psi(X)$ is related to the pupil plane field $\varphi(\xi)$ by

$$\psi(X)=N_0^{1/2}\frac{k}{2\pi i f}\exp\left[i\frac{k}{2f}X^2\right]\int d^2\xi e^{i(k/f)X\xi}\varphi(\xi)e^{-(\xi^2/2R^2)},$$

$$R(X)=\psi(X)\psi^*(X). \tag{A1}$$

The PSF triple correlation is given by

$$\begin{aligned}\langle R(X)R(X+Y)R(X+Z)\rangle&=\langle R(X)\rangle\langle R(X+Y)\rangle\langle R(X+Z)\rangle\\&+\langle R(X)\rangle|\langle\psi(X+Y)\psi^*(X+Z)\rangle|^2\\&+\langle R(X+Y)\rangle|\langle\psi(X)\psi^*(X+Y)\rangle|^2\\&+\langle R(X+Z)\rangle|\langle\psi(X)\psi^*(X+Y)\rangle|^2\\&+2\langle\psi(X)\psi^*(X+Y)\rangle\langle\psi(X+Y)\psi^*(X+Z)\rangle\\&\times\langle\psi(X+Z)\psi^*(X)\rangle.\end{aligned} \tag{A2}$$

In deriving this the assumed Gaussian statistics for the pupil plane fields was used. The terms in this expression are the five features A, B, C, and D (twice in that order) explicitly show their statistical origin. We have modeled the atmospheric distortions by a single scale Gaussian correlation function

$$\langle\varphi(0)\varphi^*(\xi)\rangle=\exp[-4\xi^2/l^2]$$

$$\langle\psi(X)\psi^*(X+Y)\rangle=\frac{N_0k^2l^2R^2}{16f^2}\times e^{-(k^2R^2Y^2/4f^2)}e^{-(k^2l^2/64f^2)(X+Y)^2}\quad\text{for } R\gg l. \tag{A3}$$

For the pupil plane fields, which are assumed to be Gaussian random fields, higher order correlations have been broken down in terms of second order correlations with the help of the well known pairing theorem for Gaussian random variables (Reed, 1962). Since the random pathlength deviation for an individual ray is believed to be hundreds of wavelengths, in the pairing theorem every pair must have one field and one conjugate field (one starred and one without). In principle, pairs like $\psi_1\psi_2$ exists but are exponentially small. Thus for the assumed statistics of the fields we get the average PSF triple correlation

$$\begin{aligned}T_R(Y,Z)&=\int d^2X\langle R(X)R(X+Y)R(X+Z)\rangle\\&=\frac{N_0^3k^4l^4R^6}{32^8f^4}\{e^{-(k^2l^2/24f^2)(Y^2+Z^2-YZ)}\\&+e^{-(k^2R^2/2f^2)(Y-Z)^2}e^{-(k^2l^2/96f^2)(Y+Z)^2}\\&+e^{-(k^2R^2/2f^2)Z^2}e^{-(k^2l^2/96f^2)(4Y^2+Z^2-4YZ)}\\&+e^{-(k^2R^2/2f^2)Y^2}e^{-(k^2l^2/96f^2)(4Z^2+y^2-4YZ)}\\&+2e^{-(k^2R^2/2f^2)(Y^2+Z^2-YZ)}e^{-(k^2l^2/96f^2)(Y^2+Z^2-YZ)}\}.\end{aligned} \tag{A4}$$

We see that the triple correlation for the binary is made of seven PSFTCs whose strengths and locations are shown in Fig. 2. The variance on the parity statistics can be represented by a diagramatic rule (Karbelkar, 1990b). The exact evaluation of all the orders is a tedious task and also unnecessary in many cases. We have considered three weight functions which emphasize three kinds of features in the triple correlation. The weight function of the first kind emphasizes the E-feature which is the true triple correlation feature. For this weight function we have already worked out the variance in detail up to all orders. This calculation (Karbelkar, 1990a), although based on a simple model of PSF, tells us that below 13th magnitude the dominant variance is in the third order in the intensity. Thus we restrict ourselves to the third order intensity calculations for feature E. The weight function of the second kind, which emphasizes all the correlation ridges, needs variance calculations up to all orders and this we do using a simpler PSF model. The weight function of the third kind emphasize the plateau region and we only set upper bounds on its SNR. The result of these approximate calculations for the weight functions of the second and the third kind shows that their SNR is poorer than that due to the main feature (E) for binaries near the diffraction limit of the telescope. For this reason it is not necessary to calculate the variance for these weight functions on the basis of detailed field calculations. So in what follows we calculate the signal for all the weight functions on the basis of detailed field calculations which take into account the edge effects. Also for the weight function of the first kind we calculate the variance as well but only in the lowest third order in the intensity.

A.1. SNR for parity detection due to the feature E

The feature E appears at seven places with strength and the locations shown in Fig. 2. As mentioned before, out of the six

asymmetric elements it is enough to consider any two, as the others do not contain any independent information. This follows from the definition of the triple correlation. If one had chosen all the six elements then the signal will be larger by a factor 3 while the variance will be larger by a factor 9 thus giving the same SNR. This is because the three third order terms in the variance

$$2\int d^2Y d^2Z T_B(Y, Z)W(Y, Z)[W(Y, Z)+W(-Y, Z-Y) + W(-Z, Y-Z)] \quad \text{(A5)}$$

contribute equally and each one of them contributes three times what they would if only two elements were used. In general if the weight function is so chosen that there is no replication of the elements in the statistical sense then only one of the three terms survives. This is the case for our choice of weight functions of the first and the second kind. We choose the weight function of the first kind shown in Fig. 3 so that it emphasizes the feature E, in particular it has the same four-volume as the feature but is unity within this volume. This weight function is chosen to be antisymmetric so that one get a antisymmetric parity statistics. Though this weight function is designed to emphasize the feature E it will get contributions from other features as well. For example the all pervading A feature due to all the PSF units will contribute. We see that the signal is just the total contribution at the port 1 minus the total contribution at the port 2 while the variance is the total contribution at both the ports (there is a factor 2). One must multiply by the volume of the weight function and the triple correlation density. This gives us the SNR [Eq. (7)] for the weight function of the first kind.

A.2. SNR for parity detection due to the correlation ridges

As described in the text of the nine ridges containing correlation ridges only three are independent. So our choice for the weight function of the second kind is shown in Fig. 4a. As the strips 1 and 3 are statistically equivalent in the average sense we can consider every strip individually. As mentioned in the text we are interested in the asymmetry in centers of these strips with respect to the $-45°$ line passing through the flux center. When a feature like A is multiplied by the weight function we get an equivalent correlation ridge feature. Consider an equivalent feature $B(Y, Z)$ situated at the origin with the triple correlation density:

$$B(Y, Z)=\frac{N_0^3k^4l^4R^6}{32^8f^4}e^{-(k^2R^2/2f^2)(Y-Z)^2}e^{-(k^2l^2/96f^2)(Y+Z)^2}. \quad \text{(A6)}$$

It is convenient to transform to coordinates $\xi=1/2(Y-Z)$ and $\eta=1/2\,(Y+Z)$ then

$$B(\eta, \xi)=\frac{N_0^3k^4l^4R^6}{32^8f^4}e^{-(2k^2R^2/f^2)\xi^2}e^{-(k^2l^2/24f^2)\eta^2} \quad \text{(A7)}$$

where a constant Jacobian of the transformation is not relevant as SNR cannot depend on a overall constant. The four-volume of the B feature is

$$\int d^2\eta d^2\xi B(\eta, \xi)=2^{-6}\pi^2N_0^3l^2R^4. \quad \text{(A8)}$$

One can integrate the B-feature density along ξ_1, ξ_2 and η_1 direction to get the projected line density $F(\eta)$ of a B-feature:

$$F(\eta)=\frac{\pi^{1.5}N_0^3kl^3R^4}{\sqrt{3}\,2^{7.5}}e^{-(k^2l^2/24f^2)\eta^2}. \quad \text{(A9)}$$

For a B-feature with center η_c away from the jump in the weight function and strength γ the contribution to parity is given by

$$\gamma 2\eta_c w(\eta_c)\frac{\pi^{1.5}N_0^3kl^3R^4}{\sqrt{3}\,2^{7.5}}. \quad \text{(A10)}$$

The effect of the weight function is a yield equal to the central $\pm\eta_c$ part of the feature as the remaining two sides cancel each other. In Fig. 4b we show the features contained in all the strips and their distance from the jump. Summing up all contributions we thus get the contribution to the signal given by Eq. (10). The third order variance is obtained by using Eq. (A8) which gives variance due to one B-feature. This variance, however, is not relevant for objects brighter than 20th magnitude and Appendix B gives the variance for this weight function in all orders based on the approximate PSF model.

Appendix B: variance for the weight function of the second kind

In this appendix we use a simpler model (following Karbelkar, 1990a) of the PSF. First of all we consider a uniform seeing disk. Within this we consider speckle-sized pixels and assume that the intensities μ_i at the i-th pixel are statistically independent Rayleigh (exponential) variables. In this notation discretised version of the weight function of the second kind shown in Fig. 4a for the central strip alone is

$$W_{ijk}=W_{i(i+a)(i+c)}=F_a\delta_{ac} \quad F_a=\text{sign}[a_1] \quad \text{(B1)}$$

where the vector subscript represents the position of the i-th pixel which is of the speckle size. First we consider the classical sixth order variance. As mentioned in the text we let the binary shrink to a point and using the specific form (B1) of the weight function to get the classical variance

$$(\alpha_1+\alpha_2)^6\sum_{ijkl}F_{j-i}F_{l-k}[\langle\mu_i\mu_j^2\mu_k\mu_l^2\rangle-\langle\mu_i\mu_j^2\rangle\langle\mu_k\mu_l^2\rangle] \quad \text{(B2)}$$

Following Karbelkar (1990a) we assume that the intensities of the speckles are distributed according to the exponential Rayleigh statistics.

$$\langle\mu_i^n\mu_j^m\rangle=\mathcal{N}^{n+m}n!m!\delta_{ij}. \quad \text{(B3)}$$

The total number of pixels within the seeing disk is N_S. The indices i etc. are two dimensional. Their components i_1 and i_2 etc. run from $-1/2N_S^{1/2}$ to $+1/2\,N_S^{1/2}$. This range actually comes from correlations which are nonzero only within a region of the order of the seeing disk. Thus it follows that

$$\sum_{j_1}F_{j_1-i_1}=-2i_1, \quad \text{(B4)}$$

$$\sum_{ijk}F_{j-i}F_{k-i}=\frac{1}{3}N_S^3. \quad \text{(B5)}$$

This gives us the sixth order variance for the weight function of the second kind

$$\frac{8}{3} N_S^3 q^6(\mathcal{N}_1+\mathcal{N}_2)^6+4N_S^2 q^6(\mathcal{N}_1+\mathcal{N}_2)^6$$

$$\sim\frac{8}{3}N_S^3 q^6(\mathcal{N}_1+\mathcal{N}_2)^6. \quad \text{(B6)}$$

The nine fifth order terms in the variance for a general third order correlation reduce to

$$(\alpha_1+\alpha_2)^5 \sum_{ijklm} \langle \mu_i\mu_j\mu_k\mu_l\mu_m\rangle W_{ijk}[W_{ilm}+4W_{lim}+4W_{ljm}] \quad \text{(B7)}$$

when the symmetry $W_{ijk}=W_{ikj}$ of the weight function is used. This gives the fifth order variance

$$4(N_S^3+3N_S^2)q^5(\mathcal{N}_1+\mathcal{N}_2)^5\sim 4N_S^3 q^5(\mathcal{N}_1+\mathcal{N}_2)^5. \quad \text{(B8)}$$

The nineteen fourth order terms in the variance, similarly, reduce to

$$2(\alpha_1+\alpha_2)^4 \sum_{ijkl} \langle \mu_i\mu_j\mu_k\mu_l\rangle W_{ijk}[2W_{ijl}+4W_{lij}+2W_{jli}+W_{ljk}]. \quad \text{(B9)}$$

This gives the fourth order variance

$$\left(\frac{4}{3}N_S^3+84N_S^2+304N_S\right)q^4(\mathcal{N}_1+\mathcal{N}_2)^4$$

$$\sim\frac{4}{3}N_S^3 q^4(\mathcal{N}_1+\mathcal{N}_2)^4. \quad \text{(B10)}$$

The third order contribution contains six terms which reduce to

$$2(\alpha_1+\alpha_2)^3 \sum_{ijk} \langle \mu_i\mu_j\mu_k\rangle W_{ijk}[W_{ijk}+W_{jik}+W_{kij}]. \quad \text{(B11)}$$

We get the third order contribution

$$(4N_S^2+2N_S)q^3(\mathcal{N}_1+\mathcal{N}_2)^3\sim 4N_S^2 q^3(\mathcal{N}_1+\mathcal{N}_2)^3. \quad \text{(B12)}$$

Since N_S is much larger than unity one need to retain only the leading terms in the every order in q. We have considered only one strip so we must multiply by 3 to get the variance due to all the strips. This gives us the variance up to all orders

$$N_S^3(72q^6(\mathcal{N}_1+\mathcal{N}_2)^6+12q^5(\mathcal{N}_1+\mathcal{N}_2)^5+4q^4(\mathcal{N}_1+\mathcal{N}_2)^4)$$

$$+12N_S^2 q^3(\mathcal{N}_1+\mathcal{N}_2)^3. \quad \text{(B13)}$$

We see that there are two transitions. The first is when the fourth order variance takes over from the classical sixth order contribution. This happens when individual speckles receive less than one photon in an exposure. The second transition occurs when the third order contribution dominates the fourth order. This happens when the entire photon count becomes less than unity.

References

Ayers, G.R., Northcott, M.J., Dainty, J.C.: 1988, *J. Opt. Soc. Am. A* **5**, 963

Beletic, J.W.: 1988, *ESO Conference and Workshop Proceedings* No. **29**, ed. F. Merkle, p. 357

Chelli, A.: 1988, *ESO Conference and Workshop Proceedings* No. **29**, ed. F. Merkle, p. 349

Dainty, J.C.: 1974, *Monthly Notices Roy. Astron. Soc.* **169**, 631

Dainty, J.C., Greenaway, A.H.: 1979, *J. Opt. Soc. Am.* **69**, 786

Gezari, D.Y., Labeyrie, A., Stachnik, R.V.: 1972, *Astrophys. J.* **173**, L1

Goodman, J.W., Belsher, J.F.: 1976, Publ. no. RADC-TR-76-50; 1977, RADC-TR-76-382; 1977, RADC-TR-77-175 (Rome Air Development Center) Griffiss Air Force Base, New York, 13441

Hoffmann, K.H.: 1988, *ESO Conference and Workshop Proceedings* No. **29**, ed. F. Merkle, p. 357

Karbelkar, S.N.: 1988, *ESO Conference and Workshop Proceedings* No. **29**, ed. F. Merkle, p. 357

Karbelkar, S.N.: 1990a, *Astrophys. J.* **351**, 334

Karbelkar, S.N.: 1990b, *J. Opt. Soc. Am. A* (to appear)

Karbelkar, S.N.: 1990c, *Astron. Astrophys.* **238**, 475

Knox, K.T., Thompson, B.J.: 1974, *Astrophys. J.* **193**, L45

Labeyrie, A.: 1970, *Astron. Astrophys.* **6**, 85

Lohmann, A.W., Weigelt, G.P., Wirnitzer, B.: 1983, *Appl. Opt.* **22**, 4028

McAlister, H.A., Hartkoff, W.I., Bagnuolo, W.G. Jr., Sowell, J.R., Franzo, O.G., Evans, D.S.: 1988, *Astron. J.* **96**, 1431

Nisenson, P.J., Papaliolios, C.: 1983, *Opt. Commun.* **47**, 91

Reed, I.S.: 1962, *IRE Trans. Inf. Theory* **IT-8**, 194

Roddier, F.: 1988, *Phys. Rep.* **170**, 99

Weigelt, G.: 1977, *Opt. Commun.* **21**, 55

Wirnitzer, B.: 1985, *J. Opt. Soc. Am. A* **2**, 14